FLOW DETAILS AROUND PILE-GROUP GROYNES

OBAIDULLAH SAFIE

Nagoya Institute of Technology, Nagoya, Japan, obaidullah.safie1@gmail.com

AKIHIRO TOMINAGA

Nagoya Institute of Technology, Nagoya, Japan, tominaga.akihiro@nitech.ac.jp

ABSTRACT

Many pile-group groynes have been used along the Kiso and Yahagi Rivers in Japan for bank protection purposes. Obviously, the arrangement of piles in a group significantly affects downstream flow structure. However, these effects have not been sufficiently studied. In this study, flow structure and turbulence characteristics in a long downstream distance of different pile-groups were investigated. Two types of pile arrangement, namely in-line and staggered arrays, were considered. The main purpose of this study was to evaluate the performance of various pile-group groynes for velocity control along the bank. The results demonstrated significant effects of pile arrangement on both flow structure and turbulence characteristics. The staggered type caused a gradual deceleration of flow from the mainstream toward the bank, while the in-line type did not yield a smooth reduction of flow. In contrast with the in-line arrangement, the staggered type maintained the low-velocity field in a long downstream distance. Furthermore, the staggered type caused a drastic reduction in the turbulence around the structure when compared with the in-line type. Different flow structures and turbulence characteristics generated by various arrangements of piles were well simulated with a two-dimensional numerical model.

Keywords: Permeable groyne, riverbank protection, spur dike, turbulence characteristics, velocity reduction

1. INTRODUCTION

Bank erosion is one of the serious problems of open channels. A groyne is a hydraulic structure that extends from a bank into the river to control the flow direction and velocity. The presence of a groyne deflects the flow from the erodible banks to increase riverbank stability. Groynes are divided into the permeable and impermeable types. A pronounced scour hole around the tip of an impermeable groyne, which is caused by the abrupt flow deviation near the tip, is the primary concern regarding structural stability (Teraguchi, 2008; Zhang, 2008; Alauddin and Tsujimoto, 2011; Sadat, 2015). Instead, a smooth reduction of velocity from the mainstream to the bank and low turbulence around the structure are the features hoped to be obtained (Uijttewaal, 2005).

In terms of flow pattern and bed morphology around the structure, the advantages of a permeable groyne over an impermeable groyne, ranging from pile groynes (Abam, 1993; Nasrollahi et al., 2008) to bandal-like structures that consist of a pile row with upper impermeable part (Teraguchi et al., 2010; Zhang et al., 2010), are often reported in the literature (Teraguchi et al., 2011; Zhang and Nakagawa, 2008). Specifically, gradual reduction of velocity from mainstream to the bank (Alauddin and Tsujimoto, 2011), local scour reduction around structure (Zhang, 2008), and enhancement of sediment deposition for further stabilization and reclamation of the eroded bank (Nakagawa et al., 2011; Ikeda et al., 1991; Dette et al., 2004) are the main advantages of permeable groynes that are reported in the literature.

Pile groynes have been proven useful for velocity reduction along the banks (Trampenau et al., 1996; Kang et al., 2011). For sufficient flow control, applications of pile-group groynes that combine multiple rows of piles within a group exist in rivers. Many pile-group groynes have been used along the Kiso and Yahagi Rivers in Japan for bank protection purposes. An example from the Kiso River is shown in Figure 1(a). Compared to an impermeable groyne, the use of a pile-group groyne is expected to contribute in reduction of excessive acceleration of the mainstream, avoiding severe local scour, weakening of the strong flow deviation and velocity gradient around the groyne head, and decreasing the resistance in flood levels, which fulfills most of the requirements formulated for a newly designed groyne (Uijttewaal, 2005). However, few studies have been conducted on the flow characteristics around a pile-group groyne.

Ikeda et al. (1991) reported flow retardation and sediment deposition along the bank behind a pile-group groyne. However, the study considered one type of pile density in a staggered pile arrangement. Recently, Safie and Tominaga (2018; 2019) highlighted the effects of the arrangement type of the piles on the flow and bed characteristics. These authors found that a pile-group with a staggered arrangement of piles outperformed an in-line arrangement. The staggered arrangement shows lower velocity along the bank than the in-line arrays.

Obviously, the number and type of arrangement of piles in the group affect the flow and turbulence characteristics both near the structure and at the far downstream. Nevertheless, the effects of pile-group groynes are unclear in the far downstream, which requires further investigations. This study investigated the flow structure and turbulence around different pile-group groynes. The changes in the flow are studied to far downstream (up to 14-times the groyne length) to determine the distance that will be effectively affected by a pile-group groyne. The principal aim of this research is identifying a suitable pile-arrangement type for a smooth reduction of velocity from mainstream to the bank and suppressed turbulence around the structure.

2. MATERIAL AND METHOD

To study the flow structure and turbulence around groynes, experiments were conducted on different permeable pile-group groynes. The particle image velocimetry (PIV) method was used to measure the velocities. The flume was 7.5 m long, 0.3 m wide, 0.4 m high, with a slope of 0.001 having a rectangular cross-section.

The pile-groups were made of acrylic cylinders with a diameter d_p of 0.5 cm and a height h_p of 5 cm. Length L and width W of the groynes were kept constant at 0.075 m in all the cases. Consequently, the groynes in all the cases covered the same planar area. The number of piles was changed in the fixed area in each pile-group groyne and was defined as pile density. The same number of rows and columns ($n = m$), hence the same face-to-face spacing between the piles in the x and y directions $S_x = S_y$ was kept in each pile density. Two pile densities, which are 5×5 and 7×7 piles, were considered in the groups to change the pile density. The pile density is defined as follows:

$$\lambda = d_p/((d_p + S_x) \cdot (d_p + S_y)) \tag{1}$$

Where d_p is the pile diameter and S_x and S_y are the face-to-face spacing between the piles.

Additionally, two types of pile arrangements, namely in-line (L cases) and staggered (S cases) types, were applied for each pile density. In the in-line type, each pile after the first row was located exactly behind the first row, however, in the staggered arrangement, each pile was directly placed against the flow. As an example, the in-line and the staggered arrangement types for the 7×7 pile-group (7L and 7S) are shown in Figure 1(b) and (c) respectively, and the details of all the cases are noted in Table 1.

The groynes were attached to one side of the channel. Figure 1 shows the schematic view of the groynes and the flume. The origin was selected to be the downstream edge of the groyne attached to the sidewall, as shown in Figure 1(d).

The flow conditions are shown in Table 2. The experiments were conducted under a non-submerged clear water condition. The initial water-depth h, measured just upstream of the groyne at $x/L = -1$ with reference to Figure 1(d), was set to 0.04 m with the aid of a tailgate before installation of a structure in the flume.

The velocities were measured by the PIV method. For visualization of the flow, nylon resin particles (80 μm diameter and 1.02 in specific weight) were used. A 3 mm green laser light sheet was projected on horizontal (x-y) planes. For each case, seven layers were recorded from the bed to the surface with a 5 mm increment. A high-speed video camera took the visual images with 200 frames in a second, and they were recorded as Audio Video Interleaved (AVI) files with 1024 × 1024 pixels. Each pixel had a side dimension of 0.03 cm. Commercial PIV software (FlowExpert by Katokoken) was used for analyses. Time-averaged velocity vectors were obtained by processing 3200 successive images in 16 seconds. The averaging time of 16 s was confirmed to be sufficient to obtain steady time-average values by comparing with 50 s data.

For nomenclature purposes, each case name begins with a number indicating the number of rows and columns, combined with the letter L or S for in-line or staggered type, respectively. For instance, Case 5L represents a pile-group of 5×5 in-line, and Case 5S is named for the 5×5 staggered. The flow of one experiment when no structure was installed in the channel, Case NoM, was also recorded, as noted in Table 1. Case NoM was considered to capture and compare the changes in the flow that occurred by the installation of a groyne in the channel.

Table 1. Details of the groynes

Case No.	Pile-group (row × column) ($n \times m$)	Case name	Number of piles in a group	Pile spacing $S_x = S_y$ (cm)	Pile density λ (1/cm)
1	5×5 In-line	5L	25	1.25	0.163
2	7×7 In-line	7L	49	0.67	0.365
3	5×5 Staggered	5S	23	1.25	0.163
4	7×7 Staggered	7S	46	0.67	0.365
5	No structure	NoM	-	-	-

Table 2. Experimental conditions for PIV experiment

Discharge Q (m³/s)	Flow Depth h (m)	Channel Slope S	Mean Velocity U_0 (m/s)	Reynolds No. Re=U_0h/ν (×10³)	Froude No. Fr
0.0016	0.04	0.001	0.13	5.3	0.21

(a) Pile-group groyne, Kiso River, Japan   (b) In-line Case 7L   (c) Staggered Case 7S
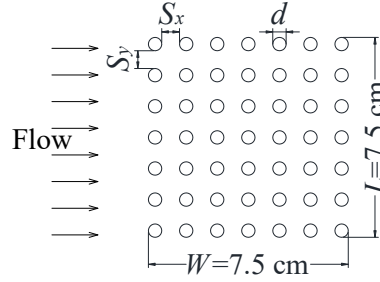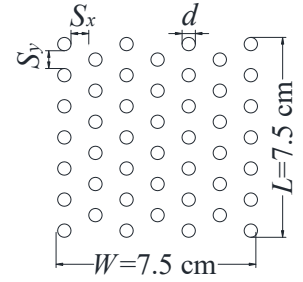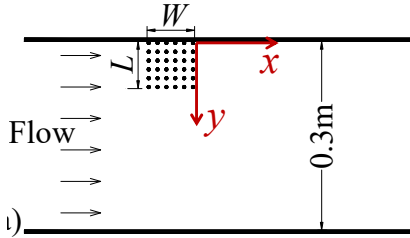
(d) Plan view of the channel   (e) Side view of the channel
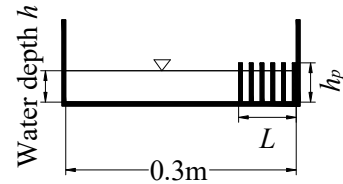
Figure 1. Pile-group layouts.

3. RESULTS AND DISCUSSION

3.1 Vertical profiles of longitudinal velocity

In this study, flow characteristics are studied from the bed to the water surface. Figure 3 shows the vertical profiles of averaged longitudinal velocity U_w, which is normalized by mean velocity U_0. The velocity U_w is averaged behind the length L of the pile-group at the section x/L=1 and is defined by Equation 2.

$$U_w(x,z) = \frac{1}{L}\int_0^L U(x,y,z)dy \tag{2}$$

Where, U is the time-averaged longitudinal velocity and z indicates the vertical direction. From Fig.4, it is clear that the presence of the piles caused a milder velocity gradient over the vertical direction in comparison with the no structure condition (Case NoM), which is consistent with the findings of Ikeda et al. (1991).

3
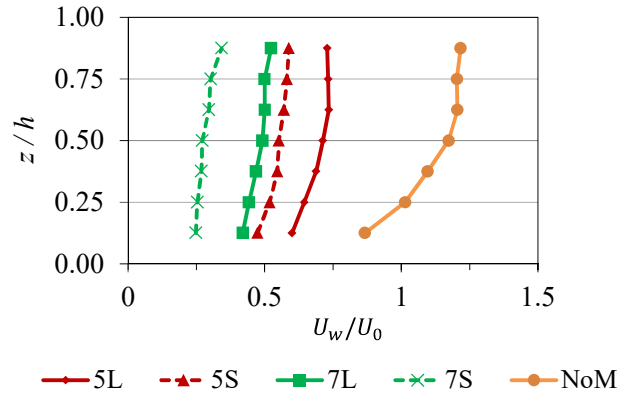
Figure 2. Vertical profiles of longitudinal velocity in the downstream of the groynes, at x/L=1.

Permeable pile groynes give rise to a rather uniform velocity profile in a non-submerged condition since the effect of the piles is present over the full water depth, which represents the rather two-dimensional nature of the flow (Uijttewaal, 2005). The change of the flow velocity and planar flow structures was small in the vertical direction downstream of the pile group. Therefore, to express the planar flow structure, depth-averaged data are used to show the results in the present study.

3.2 Depth-averaged velocity and turbulence characteristics

Figure 3 shows the depth-averaged longitudinal (U / U_0), transvers (V / U_0) and resultant (U_r / U_0) velocities, which are normalized by the mean velocity. U_r is the resultant velocity in the horizontal (x-y) plane. According to the figures, the flow was from left to right. Based on the Figure 3, the permeability of pile-group groynes resulted in a unidirectional flow toward the downstream. In both types of the pile arrangements, by increasing the pile density, the number of obstacles increases against the flow, hence the flow in the mainstream accelerated, and that behind the pile-group decelerated, as shown in Figure 3(a). By increasing the pile density, the flow deviation becomes stronger, as shown in Figure 3(b). Additionally, the staggered type shows larger flow deviation compared to an in-line groyne of the same pile density.

Changing the arrangement of piles from in-line to staggered type further decelerated the flow behind the groyne. In addition, staggered type produced a favorable change in the downstream flow pattern; a gradual smooth reduction of the velocity from the mainstream to the bank. For further clarification, Figure 4(a) shows the longitudinal velocity profiles in the lateral direction at the downstream section $x/L = 1$. The horizontal axis shows the width of the channel and the pile-group length covered from 0 to 1, as it is shaded with blue color in the figure. In the staggered cases, the flow velocity is minimized near the bank and gradually increases toward the mainstream. In contrast, the in-line cases show a high velocity near the bank; then it decreases toward the mainstream; finally, it drops to a minimum value behind the tip of the structure, at $y/L = 1$. Then, it shows a sudden jump from the minimum to maximum velocity after this point.

Figure 4(b) shows that the flow deviation occurred around the upstream tip of the pile-groups at x/L=-1. By increasing the pile density, the flow deviation became stronger. Although the arrangement type does not show a significant difference between the pile-groups with the same pile density at x/L=-1, but the staggered type shows larger transverse velocity beyond this point in comparison with the in-line type.

Besides the flow magnitude and structure, the downstream turbulence is also strongly influenced by the type of pile arrangement. Figure 5 shows the contours of Reynolds stress $-\overline{uv}/U_0{}^2$, where u and v are the velocity fluctuations in the longitudinal and transverse directions, respectively. Figure 5 represents a dramatic difference in the turbulence between both types of pile arrangements. By increasing the pile density, a region of intense turbulence appeared in the downstream of the in-line type, whereas the staggered type did not generate such strong turbulence. With reference to the longitudinal velocity profiles in Figure 4(a), the in-line cases have a minimum velocity at the downstream behind the tip of the structure at y/L=1, then there is a sudden jump to maximum velocity in the mainstream. Therefore, abrupt change of velocity from a minimum to a maximum value created a steep velocity-gradient and contributed to the generation of high turbulence along the shear layer in the in-line cases.

(a) Longitudinal velocity   (b) Transverse velocity   (c) Resultant velocity
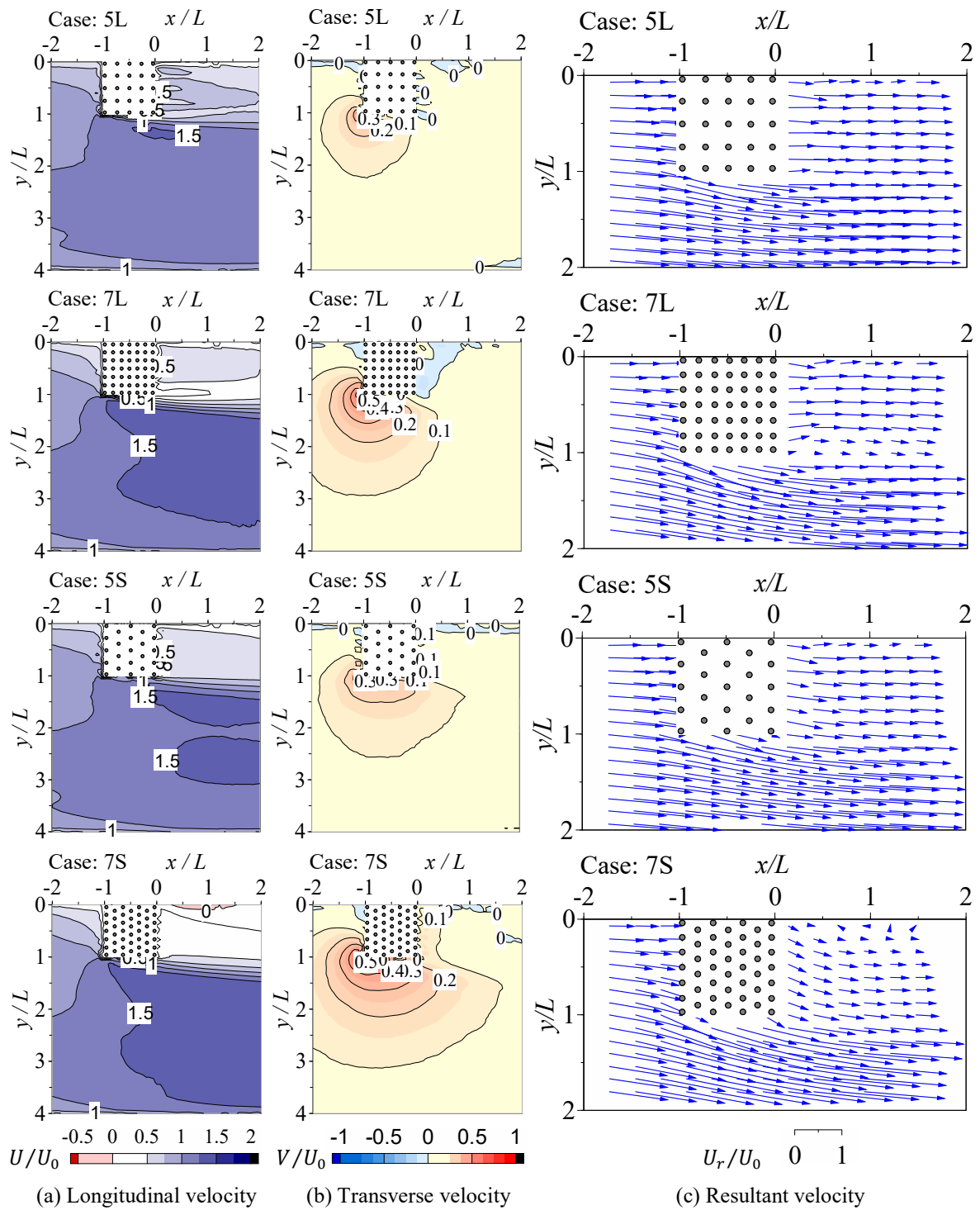
Figure 3. Depth-averaged velocities.

(a) Longitudinal velocities at $x/L=1$ (a) Transverse velocities at $y/L=1$
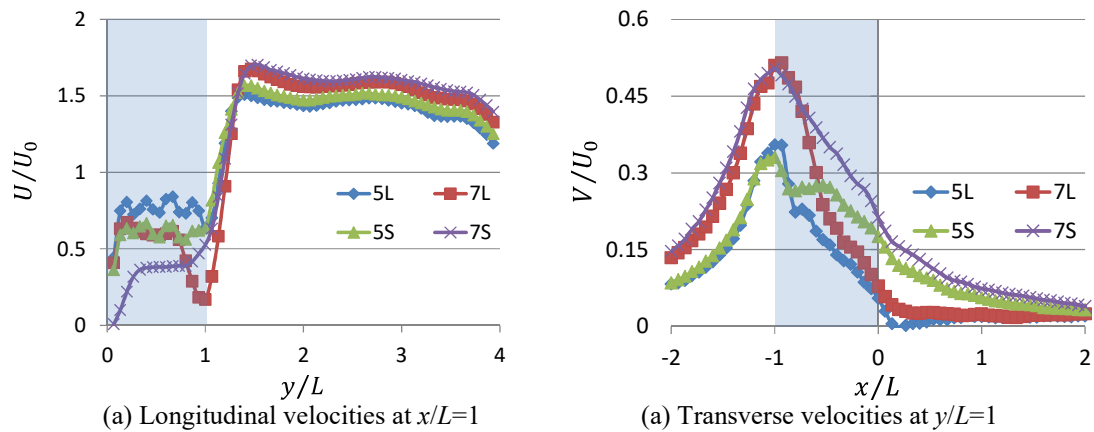
Figure 4. Depth-averaged velocity profiles.
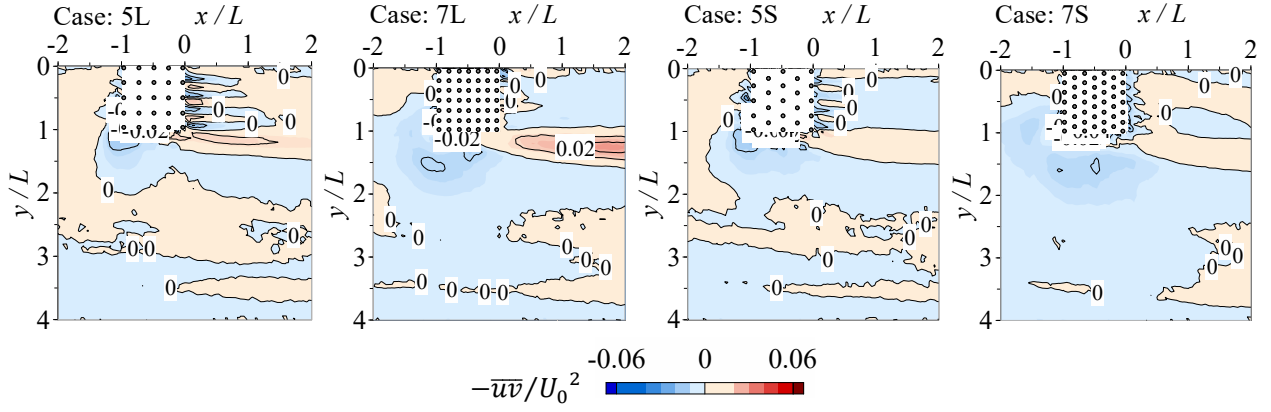
Figure 5. Depth-averaged Reynolds stress.

4. NUMERICAL CALCULATION OF THE VELOCITY

A two-dimensional depth-averaged numerical calculation with a low Reynolds-number turbulence model was conducted to simulate the effects of the pile-group groynes on the flow characteristics. The momentum and continuity equations are as follows:

$$\frac{\partial hu}{\partial t} + \frac{\partial huu}{\partial x} + \frac{\partial huv}{\partial y} = -gh\frac{\partial H}{\partial x} - \frac{\tau_{bx}}{\rho} + \frac{1}{\rho}\frac{\partial h\tau_{xx}}{\partial x} + \frac{1}{\rho}\frac{\partial h\tau_{xy}}{\partial y} \tag{3}$$

$$\frac{\partial hv}{\partial t} + \frac{\partial huv}{\partial x} + \frac{\partial hvv}{\partial y} = -gh\frac{\partial H}{\partial y} - \frac{\tau_{by}}{\rho} + \frac{1}{\rho}\frac{\partial h\tau_{xy}}{\partial x} + \frac{1}{\rho}\frac{\partial h\tau_{yy}}{\partial y} \tag{4}$$

$$\frac{\partial h}{\partial t} + \frac{\partial hu}{\partial x} + \frac{\partial hv}{\partial y} = 0 \tag{5}$$

where u and v are the depth-averaged longitudinal velocity, h is the water depth, ρ is the water density. τ_{bx} and τ_{by} are the bed shear stress in x and y directions, respectively. τ_{xx}, τ_{xy} and τ_{yy} are the depth-averaged Reynolds stresses. Bed shear stresses are expressed as follows using Manning formula and the depth-averaged Reynolds stress is expressed by means of the eddy viscosity model. The eddy viscosity in the low-Reynolds number model of Launder and Sharma (1974) is expressed as follows:

$$\nu_t = C_\mu f_\mu \frac{k^2}{\varepsilon} \quad , \quad f_\mu = \exp\left(\frac{-3.5}{1 + R_t/50}\right) \quad , \quad R_t = \frac{k^2}{\nu\varepsilon} \tag{6}$$

where C_μ is the model constant (=0.09 in the standard k-ε model), k is the depth-averaged turbulent kinetic energy, ε is the depth-averaged viscous dissipation rate. f_μ is the model function. The depth-averaged k and ε equations are calculated through the following transport equations:

$$\frac{\partial hk}{\partial t} + \frac{\partial huk}{\partial x} + \frac{\partial hvk}{\partial y} = \frac{\partial}{\partial x}\left(\frac{\nu_t}{\sigma_k}\frac{\partial hk}{\partial x}\right) + \frac{\partial}{\partial y}\left(\frac{\nu_t}{\sigma_k}\frac{\partial hk}{\partial y}\right) + P_h + P_k - h(\varepsilon + D) \tag{7}$$

$$\frac{\partial h\varepsilon}{\partial t} + \frac{\partial hu\varepsilon}{\partial x} + \frac{\partial hv\varepsilon}{\partial y} = \frac{\partial}{\partial x}\left(\frac{\nu_t}{\sigma_\varepsilon}\frac{\partial h\varepsilon}{\partial x}\right) + \frac{\partial}{\partial y}\left(\frac{\nu_t}{\sigma_\varepsilon}\frac{\partial h\varepsilon}{\partial y}\right) + \frac{\varepsilon}{k}\left(C_{\varepsilon 1}f_1 P_h - C_{\varepsilon 2}f_2 h\varepsilon\right) + P_\varepsilon + E \tag{8}$$

$$f_1 = 1.0 \quad , \quad f_2 = 1.0 - 0.3\exp(-R_t^2) \tag{9}$$

$$D = 1.85\nu\left\{\left(\frac{\partial\sqrt{k}}{\partial x}\right)^2 + \left(\frac{\partial\sqrt{k}}{\partial y}\right)^2\right\} \quad , \quad E = 2\nu\nu_t\left(\frac{\partial U_i}{\partial x_j}\right)^2 \tag{10}$$

where P_h is the production of turbulent kinetic energy, P_k and P_ε are the production source from the bed shear. f_1 and f_2 are the model functions. D and E in the above equations are additive terms in the low-Reynolds number model. The other model constants are the same as the standard model, as shown in Table 3.

Table 3. Constants in the depth-averaged k - ε model.

C_μ	σ_k	σ_ε	$C_{\varepsilon 1}$	$C_{\varepsilon 2}$
0.09	1	1.3	1.44	1.92

The measured and calculated flow characteristics are depicted in a long downstream distance of the structure in Figure 6 and 7, respectively. The flow and turbulence distributions of the measured (Figures 6) and calculated (Figure 7) results show strong agreement with each other. The long downstream results revealed another new finding that is the staggered Case 7S produced larger turbulence in the far downstream. The reason comes from the velocity gradient along the shear layer. The contour lines along the shear layer are wider in the Case 7L compared to the 7S at the section x / L =13.5. It represents the existence of a higher velocity gradient in the far downstream of the 7S. Consequently, Case 7S produced larger turbulence in the far downstream compared to the in-line Case 7L. However, the calculated results (Figure 7) shows that the high turbulence located close to the pile-group in the Case 7L, although the experimental result (Figure 6) shows some distance to the downstream. Numerical calculations require further improvements.

(a) Longitudinal velocity　　　　　　　　　　(b) Reynolds stress
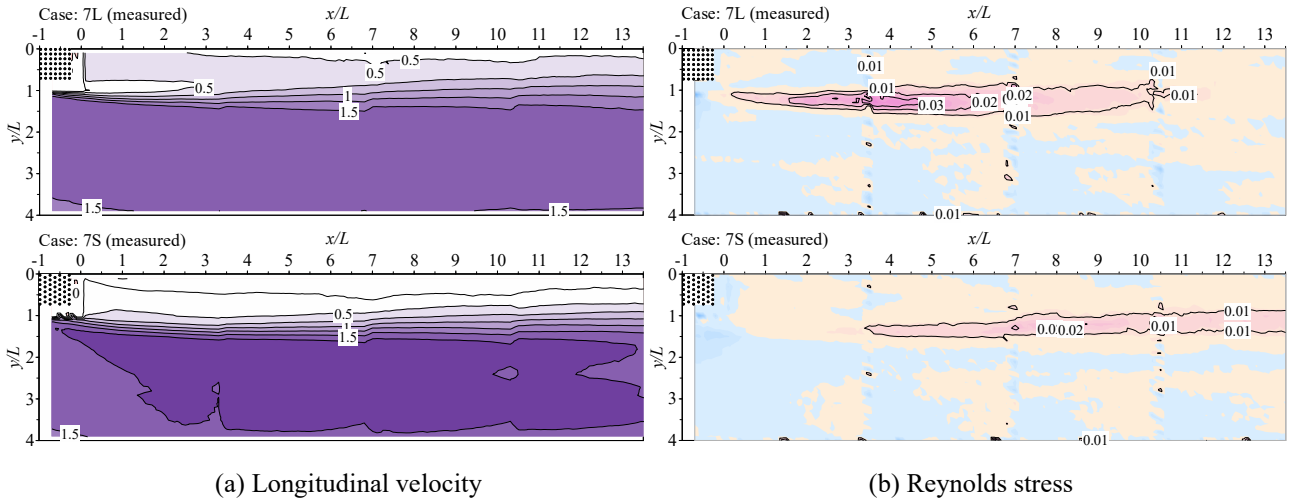
Figure 6. Results of laboratory experiments

(a) Longitudinal velocity　　　　　　　　　　(b) Reynolds stress
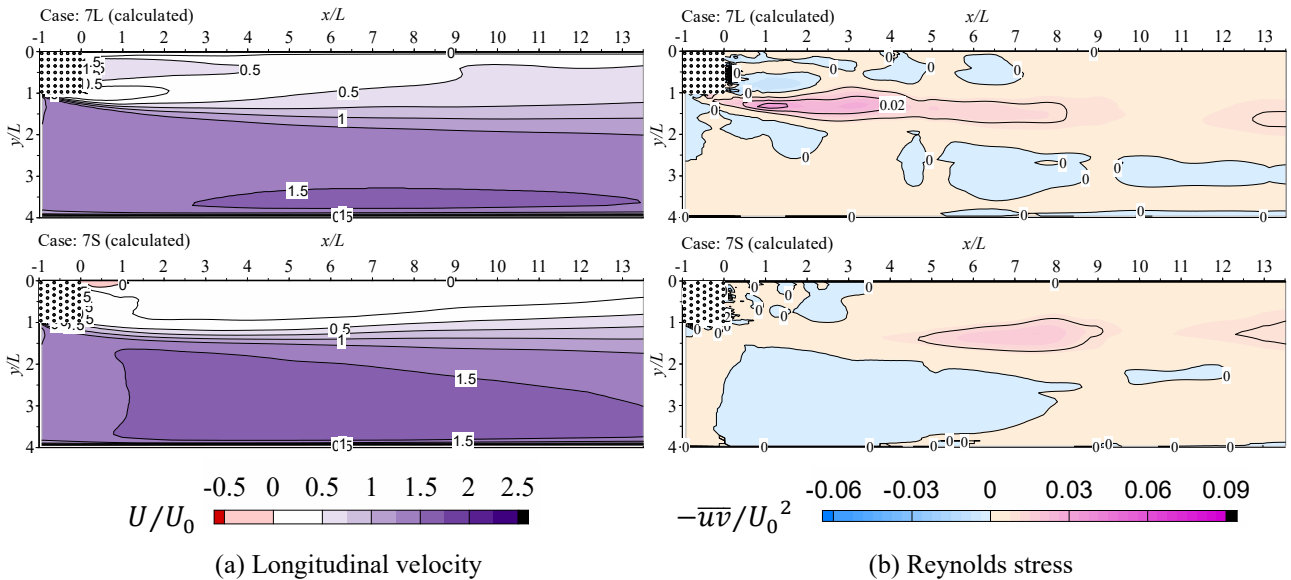
Figure 7. Results of numerical calculations

5. CONCLUSIONS

The effects of pile density and arrangement on the flow characteristics around pile-group groynes were investigated. This research was aimed at identifying an efficient design of pile arrangement in a pile-group groyne to produce a smooth flow reduction with low turbulence around the structure for riverbank protection. The main conclusions from this study are as follows.

The pile-group groynes effectively reduced the velocity along the bank. It was found that the type of pile arrangement within a group significantly affected the flow magnitude, pattern, and turbulence parameters. The staggered type arrangement represented improvements compared to the in-line type. The gradual reduction of velocity from the mainstream to the bank, the substantial decrease in turbulence around the structure, and preservation of the retarded flow to a far downstream distance are the main favorable features of the staggered type.

Besides the experimental study, a two-dimensional numerical calculation was conducted to simulate the effect of pile-group groynes on the flow characteristics in a long downstream of the structure. The calculated and measured results around the groynes show strong agreement with each other. A dual feature was revealed in the turbulence intensity of the most upstream and far downstream of a pile-group groyne by investigating long downstream distance affected by a groyne. This feature was reversed in the in-line and staggered types; the turbulence was suppressed at the most upstream part of the staggered type compared to the in-line type, while in the far downstream region it represented an opposite trend. Additionally, the velocity gradient was smaller at the most upstream part of the staggered type compared to the in-line type, while it was the opposite in the far downstream region. From the above feature, it was inferred that the retarded velocity maintains a long distance in the staggered type compared to the in-line arrangement.

This study revealed some unknown perspectives of the flow induced by pile-group groynes having different pile arrangements, which can be useful in practical engineering fields. However, the detailed mechanism of the turbulence generation, morphodynamic evolutions around the structure, and the effects of pile-group submergence require further investigation.

REFERENCES

Abam, T. K. S. (1993). Control of channel bank erosion using permeable groins. *Environmental Geology*, 22(1): 21-25.

Alauddin, M., and Tsujimoto, T. (2011). Optimum design of groynes for stabilization of lowland rivers. *Journal of Japan Society of Civil Engineers, Series B1 (Hydraulic Engineering),* 67(4): I_145-I_150.

Dette, H. H., Raudkivi, A. J., and Oumeraci, H. (2004). Permeable Pile Groin Fields. *Journal of Coastal Research*, SI(33): 145-159.

Ikeda, S., Izumi, N., and Ito, R. (1991). Effects of pile dikes on flow retardation and sediment transport. *Journal of Hydraulic Engineering*, 117(11): 1459-1478.

Kang, J., Yeo, H., Kim, S., and Ji, U. (2011). Permeability effects of single groin on flow characteristics. *Journal of Hydraulic Research*, 49(6): 728-735.

Launder, B. E., and Sharma, B. I. (1974). Application of the energy-dissipation model of turbulence to the calculation of flow near a spinning disc. *Letters in Heat and Mass Transfer,* 1: 131-138.

Nakagawa, H., Teraguchi, H., Kawaike, K., Baba, Y., and Zhang, H. (2011). Analysis of bed variation around bandal-like structures. *Annuals of Disaster Prevention Research Institute, Kyoto University,* 54(B): 497-510.

Nasrollahi, A., Ghodsian, M., and Salehi Neyshabouri, S. A. A. (2008). Local Scour at Permeable Spur Dikes. *Journal of Applied Sciences*, 8(19): 3398-3406.

Sadat, S. H. (2015). Modification of spur-dike with footing or pile-group to stabilize river morphology and reduce local scour, *Ph. D. thesis, Nagoya Institute of Technolgy, Nagoya, Japan.*

Safie, O., and Tominaga, A. (2018). Effect of pile arrangement on flow characteristics around pile-group dike. *Journal of Japan Society of Civil Engineers, Series A2 (Applied Mechanics)*, 74(2): I_439-I_448.

Safie, O., and Tominaga, A. (2019) : Effects of pile density and arrangement on flow characteristics and sediment deposition around a pile-group dike. *Journal of Japan Society of Civil Engineers, Series A2 (Applied Mechanics)*, 75(2): I_487-I_498.

Teraguchi, H., Nakagawa, H., Muto, Y., Baba, Y., and Zhang, H. (2008). Flow and sediment transport around impermeable or permeable groins. *Journal of Japan Society of Civil Engineers, Annual Journal of Hydraulic Engineering*, 52: 175-180.

Teraguchi, H., Nakagawa, H., Kawaike, K., Baba, Y., and Zhang, H. (2010). Morphological changes induced by river training structures: bandal-like structures and groins. *Annuals of Disaster Prevention Research Institute, Kyoto University*, 53(B): 595-605.

Teraguchi, H., Nakagawa, H., Kawaike, K., Baba, Y., and Zhang, H. (2011). Alternative method for river training works: bandal-like structutrs. *Journal of Japan Society of Civil Engineers, Series B1 (Hydraulic Engineering)*, 67(4): I_151-I_156.

Trampenau, T., Goricke, F., and Raudkivi, A. J. (1996). Permeable pile groins. *Proceedings of the 25th Conference on Coastal Engineering, ASCE, Florida, USA.*

Uijttewaal, W. S. J. (2005). Effects of groyne layout on the flow in groyne field: laboratory experiments. *Journal of Hydraulic Engineering*, 131(9): 782-791.

Zhang, H., and Nakagawa, H. (2008). Scour around spur dyke: Recent advances and future researches. *Annuals of Disaster Prevention Research Institute, Kyoto University,* 51(B): 633-652.

Zhang, H., Nakagawa, H., Baba, Y., Kawaike, K., and Teraguchi, H. (2010). Three-dimensional flow around bandal-like structures. *Journal of Japan Society of Civil Engineers, Annual Journal of Hydraulic Engineering*, 54: 175-180.

Zhang, H., and Nakagawa, H. (2009). Characteristics of local flow and bed deformation at impermeable and permeable spur dykes. *Journal of Japan Society of Civil Engineers, Annual Journal of Hydraulic Engineering*, 53: 145-150.